

Mica polytypism: similarities in the crystal structures of coexisting 1M and 2M₁ oxybiotite

TSUTOMU OHTA, HIROSHI TAKEDA AND YOSHIO TAKÉUCHI

*Mineralogical Institute, Faculty of Science
University of Tokyo, Hongo, Tokyo 113, Japan*

Abstract

The crystal structures of coexisting 1M and 2M₁ oxybiotites were refined by the X-ray diffraction method in order to examine the role of hydrogen in mica structures and polytypism. The unit-layer structures of coexisting 1M and 2M₁ oxybiotites were found to be identical within the limit of the accuracy of the structure refinement. This similarity leads to the conclusion that they are ideally polytypic in spite of the complexity of unit-layer structures such as micas.

The oxybiotites lack hydrogen and instead are enriched in ferric iron. The structural parameters of the tetrahedral and octahedral layers have been found to be remarkably similar to those of the hydrogenated structures. Comparison with hydrogenated biotite suggests that the lack of hydrogen atoms mainly affects the interlayer configuration and consequently causes the interlayer separation to decrease. This feature can be attributed to the fact that interactions between K⁺ and H⁺ are very extensive in hydrogenated biotites.

Introduction

Mica is one of the layer silicates in which hydrogen plays an important crystal chemical role. The detailed structure analysis of a trioctahedral mica was initiated by Takéuchi and Sadanaga (1959). Since then many reports have been published on the crystal structures of various mica polytypes and of various chemical compositions, and the structural changes due to cation substitutions have been discussed. For example, the dimensional misfit between the octahedral and tetrahedral layers in mica structures was treated by Radoslovich and Norrish (1962). Takéuchi (1965) compared the two brittle micas, margarite and xanthophyllite.

The structural changes of micas due to cation substitutions have been investigated by several workers (Donnay, Donnay and Takeda, 1964; Hazen and Wones, 1972). The crystal structures of micas at high temperature (Takeda and Morosin, 1975) and at high pressure (Takeda, 1977) have also been studied. Although oxygen fugacity is another important factor in crystallization of minerals in nature, its effect especially that of hydrogen on mica structures has not yet been tackled. Takéuchi (1965) suggested that the interaction between OH groups and interlayer cations could possibly be

correlated with the preference of basic polytypes in micas.

Mica structures are based on the stacking of the unit layers which comprise two tetrahedral layers sandwiching an octahedral layer, and an interlayer. Since hydrogen atoms lie nearly directly below or above the interlayer cation in the hole of tetrahedral layer, they should affect the structure of the unit layer when a unit layer stacks upon another layer. It is therefore suggested that the lack of hydrogen atoms in mica crystals also effectively changes the structure. The effect of the presence or absence of hydrogen atoms on a crystal structure is also of crystal chemical interest in general. Structural changes caused by oxidation-reduction reactions coupled with dehydrogenation-hydrogenation reactions may occur but are not well understood.

Micas have many polytypes or polymorphs. Hendricks and Jefferson (1939) studied the stacking mode of layers in micas. Amelinckx and Dekeyser (1953) attributed mica polytypism to a spiral growth mechanism and gave some stacking modes, while Smith and Yoder (1956) derived six basic regular modes of stacking and gave a nomenclature of mica polytypes, 1M, 2M₁, 2M₂, 2O, 3T and 6H. The stacking sequences of complex mica polytypes were later determined by Ross, Takeda and Wones

(1966). A complex mode of stacking sequence based on probability was recently determined by Ohta, Takéuchi and Takeda (1978) in a valuevite mica.

These numerous detailed X-ray studies have shown the high observation frequency of a limited number of short-period polytypes in micas, such as 1M, 2M₁ and 3T. This fact poses a question of whether a structural control over the layer stacking may exist during crystal growth. Such structural control forces may be provided by the interaction of interlayer cation and hydroxyl or fluorine ions, or by the neutrality of the surface oxygen rings (Takeda and Burnham, 1969; Takeda, Haga and Sadanaga, 1971) or both. Güven (1971) discussed the structural factors controlling stacking sequences in dioctahedral micas.

In order to resolve this question, it is important to examine the structural differences between the unit layers of coexisting polytypes, since the chemical compositions, temperature and pressure of crystallization can be assumed to be similar for such polytypes. Dissimilarities in the crystal structures of coexisting 1M and 2M₁ biotites (hydrogenated) were found by Takeda and Ross (1975), who discussed an origin of mica polytypism on the basis of the unit-layer constraints coupled with spiral growth mechanism. However, the structures of the oxidized counterparts have been left unsolved by these authors.

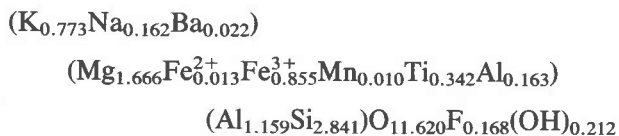
In view of these developments on mica polytypisms, in the present study we carefully refined the crystal structures of coexisting 1M and 2M₁ oxybiotites, which lack hydrogen atoms, and examined the effects of the loss or addition of hydrogen atoms on the unit-layer structures by comparing the structures of the oxybiotites with those of the hydrogenated oxybiotites determined by Takeda and Ross (1975). Comparison of the unit-layer structure of the 1M polytype with that of the 2M₁ polytype was also made for both oxidized and hydrogenated members, in order to elucidate the possible effect of stacking sequences on the exact configuration of the unit layer within the different polytypes, and the role of the hydrogen on mica polytypism.

Experimental

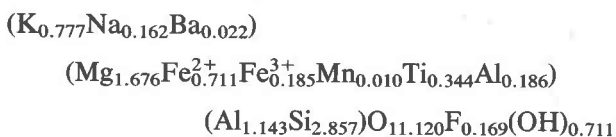
Specimen description

The oxybiotite crystals used in this study occur in a rhyodacite ash flow from Ruiz Peak area, Valles Mountains, New Mexico. The oxidation caused the biotite crystals to turn dark reddish brown. A

mineralogical description of the oxybiotite has been previously reported by Takeda and Ross (1975), who gave the chemical formula of the oxybiotite based on wet chemical analysis as follows.



The chemical formula can be compared with that of the hydrogenated oxybiotite, which was produced by adding hydrogen atoms into Ruiz Peak oxybiotite (Takeda and Ross, 1975), as below.



The main difference in the chemical composition is that the original oxybiotite contains less hydrogen and more ferric iron. The ratio of Mg/(Mg+Fe) is about 2/3.

Because of the difficulty in obtaining undeformed fragments of layer silicates, single crystals suitable for the X-ray diffraction studies have been carefully selected. A good single crystal of each of the 1M and 2M₁ form was found from more than thirty crystals examined. In addition to 1M and 2M₁ forms, more complex polytypes and twins were found among the other crystals examined. The plate of the 1M oxybiotite used for X-ray intensity measurement is 0.15 × 0.19 × 0.07 mm in size, and that of 2M₁ oxybiotite is 0.25 × 0.30 × 0.07 mm.

Crystal data

The crystals were mounted along *c** and the precession photographs of reciprocal lattice nets *h0l,0kl*, *1kl*, *hhl* and *h3hl* of the two specimens were taken with Zr-filtered MoK α radiation. The photographs of the crystals used for the structure determinations showed patterns of neither twinning nor complex stacking arrangements. The presence criteria and the symmetry of the diffraction patterns are compatible with possible space groups *C2*, *Cm* or *C2/m* for the 1M oxybiotite, and *Cc* or *C2/c* for the 2M₁ oxybiotite. The space group adopted in the final structure refinement for each mica is given in Table 1.

The cell dimensions of 1M and 2M₁ oxybiotites obtained by the present study are listed in Table 2, together with those of hydrogenated oxybiotites

Table 1. Selected crystal data* for oxybiotites 1M and 2M₁

| | Dx (gcm ⁻³) | Z | sp. gr. | μ (cm ⁻¹) |
|----------------------------|-------------------------|---|---------|-----------------------|
| oxybiotite 1M | 3.074 | 2 | C2/m | 26.86 |
| oxybiotite 2M ₁ | 3.075 | 4 | C2/a | 26.87 |

* Dx: calculated density
 Z: the number of formula units per cell
 sp. gr.: space group
 μ: linear absorption coefficient

(Takeda and Ross, 1975). The cell parameters were obtained by the least squares refinements of 15 independent reflections, measured with a 4-circle single-crystal diffractometer using MoK α radiation ($\lambda = 0.71069\text{\AA}$) with graphite-monochromator. The calculated densities, the number Z of formula units per cell, and the linear absorption coefficients are tabulated in Table 1.

Intensity measurements and data reduction

The crystals selected for the intensity measurements revealed no detectable mechanical distortion in their X-ray diffraction photographs. Such distortion, common in micas, has been known to introduce inaccuracies in the structure refinements. Intensity measurements for the specimens used in the present work were made with a Syntex P2₁ automated four-circle single-crystal diffractometer, using MoK α radiation ($\lambda = 0.71069\text{\AA}$) monochromatized by a graphite monochromator. The ω -2 θ scan technique was employed to measure intensities in the range of 2 θ less than 75° in the variable scan mode. Three standard reflections were monitored every 100 reflections during the measurements. The intensities of reflections with the indices *hkl* and $\bar{h}kl$ were measured for 1M and 2M₁ oxybiotites. Integrated intensities were corrected for Lorentz and polarization effects and were reduced to structure factors |F_o|. The absorption correction then was made by the ACACA program (Wuensch and Prewitt, 1965) with the linear absorption coefficient listed in Table 1 for each crystal.

Structure refinements

Oxybiotite 1M

The reflections for which $I \geq 2\sigma(I)$ were considered to be observed, and 1125 nonequivalent reflections were utilized in the following refinement. The structure refinement was carried out using the full-matrix least-squares refinement program in the

MINEPAC system (Miyamoto *et al.*, 1974) and also using program LINUS (Coppens and Hamilton, 1970). The atomic scattering factors used with MINEPAC were taken from Cromer and Mann (1968), and those used with LINUS from the *International Tables for X-ray Crystallography Vol. IV* (1974), the oxygen atoms being considered half-ionized and all cations completely ionized. Anomalous dispersion corrections were made by using the coefficients taken from the above table. The weights used in refinement are $1/\sigma(F_o)^2$, where $\sigma(F_o)$ is the standard deviation of |F_o|. The space group C2/m was assumed and turned out to be correct on the refinement.

The refinement of 1M oxybiotite was initiated by using the positional parameters and isotropic temperature factors of hydrogenated 1M biotite (Takeda and Ross, 1975). The distribution of cations was assumed to be disordered. The adjustment of scale for F_o and F_c gave the conventional R value equal to 16.2%. After 3 cycles of refinement of atomic coordinates, convergence was obtained (R = 10.9%). Three more cycles of refinement of atomic coordinates and isotropic temperature factors resulted in convergence to the R value of 9.2%. During these cycles of refinement, the y coordinate of the M2 site shifted by over twenty times the standard deviation for the parameter from the initial position, in contrast with the other parameters which shifted by less than ten times the standard deviations. In addition to this change, the isotropic temperature factor for the M1 site (1.35) was significantly different from that for the M2 site (0.76). The fact implies that the M1 site may be more Mg-rich than the M2 site. Three cycles of refinement of the anisotropic temperature factors together with the atomic coordinates resulted in convergence to R = 5.4%. The refinement of the site occupancy factors was then carried out.

Table 2. Cell parameters of oxybiotites and hydrogenated oxybiotites from Ruiz Peak, New Mexico

| setting | a (Å)* | b (Å) | c (Å) | β (°) | v (Å ³) |
|---------------------------------|-----------|----------|-----------|------------|---------------------|
| oxybiotite | | | | | |
| 1M 1M | 5.3204(6) | 9.210(1) | 10.104(1) | 100.102(8) | 487.46(9) |
| 2M ₁ 2M ₁ | 5.3175(7) | 9.212(2) | 19.976(3) | 95.09(1) | 974.7(3) |
| 2M ₁ 1M** | 5.3183 | 9.211 | 10.105 | 100.09 | 487.4 |
| hydrogenated oxybiotite | | | | | |
| 1M 1M | 5.331(2) | 9.231(4) | 10.173(4) | 100.16(3) | 492.8 |
| 2M ₁ 2M ₁ | 5.329(2) | 9.234(3) | 20.098(7) | 95.09(3) | 985.1 |
| 2M ₁ 1M** | 5.331 | 9.231 | 10.168 | 100.14 | 492.6 |

* Error in parentheses.

** Unit-cell parameters of the unit layer of the 2M₁ biotite in the 1M setting.

Manganese and ferrous iron have atomic scattering factors similar to those of ferric iron, and are minor elements in the oxybiotite. Thus, the contributions of manganese and ferrous iron were conveniently assumed to be the same as that of ferric iron. The preliminary refinement of the site occupancies were made for Mg and Fe and also for Ti and Al between the *M1* and *M2* sites. Several cycles of refinements showed that Mg and Al were enriched in the *M1* site ($R = 4.4\%$, $wR = 5.35\%$) in accord with the tendency deduced from the isotropic temperature factors mentioned in the previous paragraph. The refinement up to this stage was carried out using the MINEPAC program system, and then the program LINUS was used for the subsequent refinement.

During the course of the site occupancy refinement, the following physical and chemical constraints were applied as developed by Finger (1969): (1) the total fractional occupancy of a site must equal 1.0 and (2) the site chemistry must agree with the bulk chemistry. The derivatives were modified with the use of these constraints.

It may be possible for Fe^{3+} and Ti to occupy tetrahedral sites. There is one tetrahedral site, *T*, and two octahedral sites, *M1* and *M2*, in the 1M polytype in space group *C2/m*. Silicon occupies only the *T* site. Hence, the occupancy factors to be refined are those of Al, Fe and Ti for *T* site, and Mg, Fe, Ti and Al for *M1* and *M2* sites. Since Ti and Fe have similar scattering factors as do Mg and Al, simultaneous refining of the site occupancies of these cations was not successful. Such site occupancy refinement gives rise to very high correlation coefficients between the parameters refined. Thus, the site occupancies were refined step by step as described below.

As a first trial, the occupancy of Fe^{3+} in the *T* site was estimated. In this refinement, Al was treated as Mg, because of the similarity in their scattering factors, and Ti was assumed not to occupy the *T* site. During the refinements, the occupancy parameters of Mg in *M1*, Fe in *M2* and *T* were allowed to vary. The other occupancy parameters were obtained by the chemical constraints mentioned above. Two cycles of refinements reduced residual *R* to 4.4% and revealed that a part of the *T* site was occupied by Fe^{3+} and that the *M1* site was not occupied by Ti. The same result has been obtained by refining the Ti occupancy in the *T* site. Therefore, Ti was assumed to occupy the *M2* site in the subsequent refinements. The occupancy factors of

Mg in *M2* and Fe in *T* were refined again, and the values thus obtained were fixed in the following run.

After the readjustment of the occupancy factors of Mg and Fe in the octahedral sites, the amount of Mg and Al were estimated, fixing all other parameters determined previously. By varying the occupancy factors of Mg in *M1*, convergence was achieved, although the estimated standard deviation of the varied parameter was large and was about 0.1 in fractional occupancy.

Isotropic extinction correction was made with LINUS. Two cycles of refinement introduced no significant improvement of the value of *R*. After three cycles of refinement, during which the scale factor, the atomic coordinates, the anisotropic temperature factors, the isotropic extinction coefficient and the occupancy factor for Mg and Fe in the *M1* and *M2* sites were varied, no further change of parameters took place. The final conventional unweighted residual and the weighted one were 4.4% and 5.0% respectively. The observed and calculated structure factors are listed in Table 3a.¹

Oxybiotite 2M₁

The structure refinement was carried out using the program LINUS in a way similar to the refinement of the oxybiotite 1M structure. Of the intensities measured, 1676 nonequivalent reflections with $I \geq 2\sigma(I)$ were used in the refinement. Space group *C2/c* was assumed in the following refinement and turned out to be correct. The refinement in *Cc* was also carried out but did not show any evidence for preference of *Cc* to *C2/c*. The atomic coordinates and isotropic temperature factors of the 2M₁ hydrogenated oxybiotite (Takeda and Ross, 1975) were used as starting parameters for the 2M₁ oxybiotite. After seven cycles of isotropic refinement ($R = 7.7\%$) anisotropic temperature factors were included and convergence was achieved in an additional three cycles ($R = 5.1\%$).

The method of site occupancy refinements was similar to that employed for the 1M oxybiotite, except for the following difference. All silicons were distributed equally over the two nonequivalent tetrahedral sites, *T1* and *T2*. The scale factor, the atomic coordinates, the anisotropic temperature

¹To receive a copy of Table 3a and 3b, order Document AM-82-198 from the Business Office, Mineralogical Society of America, 2000 Florida Avenue, N.W., Washington, D. C. 20009. Please remit \$1.00 in advance for the microfiche.

factors, the occupancy parameters for Si and Al in tetrahedral sites and those for Mg and Fe in octahedral sites, and the isotropic extinction coefficient were refined in the final five cycles. The final unweighted conventional residual is 3.9% and the weighted one 4.5%. The observed and calculated structure factors are listed in Table 3b.

Results

The atomic coordinates and anisotropic temperature factors for the 1M and 2M₁ oxybiotites are presented in Table 4a, 4b, and 4c. The observed coordinates of the unit layer of the 2M₁ polytype in the 1M setting are compared in Table 4a with the observed 1M coordinates. The transformation of the 2M₁ coordinates to the 1M setting was performed by the same procedure as that for the 2M₁ hydrogenated oxybiotite (Takeda and Ross, 1975).

The results of the site occupancy refinements are listed in Table 5. The various bond lengths, selected bond angles and associated standard deviations (Table 6) were computed from the atomic positions by the ORFFE program (Busing, Martin and Levy, 1964). The variance-covariance matrix of the final refinement and the standard deviations of the unit-cell parameters were used for these computations. The magnitudes and orientations of thermal ellipsoids (Table 7) are also calculated by ORFFE. The projections of the structures on (001) of the unit

Table 4a. Atomic coordinates of oxybiotites 1M and 2M₁ in the 1M setting*

| Atom** | Form | x | y | z |
|--------|-----------------|-----------|------------|------------|
| M1 | 1M | 0.0 | 0.0 | 0.5 |
| M1 | 2M ₁ | -0.00005 | -0.00005 | 0.5000 |
| M2 | 1M | 0.0 | 0.34538(9) | 0.5 |
| M2 | 2M ₁ | 0.0001 | 0.34513 | 0.5000 |
| K | 1M | 0.0 | 0.5 | 0.0 |
| K | 2M ₁ | 0.0 | 0.5 | 0.0 |
| T | 1M | 0.0730(1) | 0.16733(8) | 0.22283(7) |
| T1 | 2M ₁ | 0.0732 | 0.16733 | 0.22299 |
| T2 | 2M ₁ | 0.0731 | 0.16734 | 0.22286 |
| O1 | 1M | 0.0177(6) | 0.0 | 0.1666(3) |
| O11 | 2M ₁ | 0.0167 | 0.0003 | 0.1671 |
| O2 | 1M | 0.3217(4) | 0.2315(2) | 0.1645(2) |
| O21 | 2M ₁ | 0.3223 | 0.2315 | 0.1647 |
| O22 | 2M ₁ | 0.3221 | 0.2309 | 0.1651 |
| O3 | 1M | 0.1298(3) | 0.1697(2) | 0.3905(2) |
| O31 | 2M ₁ | 0.1287 | 0.1698 | 0.3905 |
| O32 | 2M ₁ | 0.1288 | 0.1691 | 0.3907 |
| O4 | 1M | 0.1335(5) | 0.5 | 0.4006(3) |
| O4 | 2M ₁ | 0.1324 | 0.4998 | 0.4001 |

* Both forms are listed in the 1M setting to facilitate comparison. The atomic coordinates for the 2M₁ polytype in the 2M₁ setting are given in Table 4b.

** Standard deviations for the 1M form are given in parentheses: those of the 2M₁ form are listed in Table 4b.

Table 4b. Atomic coordinates of oxybiotite 2M₁ in the 2M₁ setting

| Atom* | x | y | z |
|-------|-----------|------------|-------------|
| M1 | 0.75 | 0.25 | 0.0 |
| M2 | 0.2321(1) | 0.07750(7) | -0.00001(3) |
| K | 0.0 | 0.0832(1) | 0.25 |
| T1 | 0.4624(1) | 0.24902(9) | 0.13850(4) |
| T2 | 0.9645(1) | 0.4163(1) | 0.13857(4) |
| O11 | 0.7421(4) | 0.3139(2) | 0.1664(1) |
| O21 | 0.2416(4) | 0.3512(2) | 0.1677(1) |
| O22 | 0.4352(4) | 0.0822(2) | 0.1675(1) |
| O31 | 0.4309(3) | 0.2477(3) | 0.05473(9) |
| O32 | 0.9392(3) | 0.4172(3) | 0.05466(9) |
| O4 | 0.9333(3) | 0.0827(3) | 0.04994(9) |

* Estimated standard deviations are given in parentheses and are expressed in units of last digit stated.

layers for the 1M and 2M₁ oxybiotites (Fig. 1 and Fig. 2) are drawn with the ORTEP program (Johnson, 1965).

In order to elucidate the effect of the loss or addition of hydrogen on mica structures, it is necessary to compare various layer thicknesses in a unit layer. Let us define the *d* values representing various layer thicknesses (Fig. 3) as follows:

d(*u*) represents unit-layer thickness, *d*(*u*) = *d*(001) for the 1M polytype and *d*(*u*) = *d*(001)/2 for the 2M₁ polytype;

Table 4c. Anisotropic temperature factors* $\beta_{ij} \times 10^4$ and equivalent isotropic temperature factors *B* of Ruiz Peak oxybiotites

| Atom | β_{11} | β_{22} | β_{33} | β_{12} | β_{13} | β_{23} | <i>B</i> _{equiv.} |
|----------------------------|--------------|--------------|--------------|--------------|--------------|--------------|----------------------------|
| oxybiotite 1M | | | | | | | |
| M1 | 40(4) | 12(1) | 33(1) | 0 | 12(2) | 0 | 0.71 |
| M2 | 33(2) | 28.6(9) | 30.8(7) | 0 | 7.3(9) | 0 | 0.85 |
| K | 167(5) | 53(2) | 75(2) | 0 | 23(2) | 0 | 2.19 |
| T | 45(2) | 15.8(6) | 31.3(6) | 0.4(9) | 8.7(8) | 0.1(6) | 0.75 |
| O1 | 146(10) | 26(3) | 41(3) | 0 | 6(4) | 0 | 1.39 |
| O2 | 98(6) | 44(2) | 40(2) | -19(3) | 17(3) | -5(2) | 1.37 |
| O3 | 49(5) | 15(2) | 31(1) | 1(2) | 11(2) | -1(1) | 0.75 |
| O4 | 57(7) | 22(2) | 30(2) | 0 | 10(3) | 0 | 0.84 |
| oxybiotite 2M ₁ | | | | | | | |
| M1 | 51(3) | 15(1) | 7.1(3) | 0 | 1.4(6) | 0 | 0.74 |
| M2 | 77(2) | 18.6(6) | 6.8(1) | 16 | 0.0(4) | 0.9(3) | 0.86 |
| K | 164(3) | 56(1) | 17.8(3) | 0 | 4.3(8) | 0 | 2.19 |
| T1 | 46(3) | 15(1) | 6.5(3) | 3(1) | 0.7(4) | 0.0(4) | 0.69 |
| T2 | 49(3) | 17(1) | 6.3(2) | 3(1) | 0.3(4) | 0.4(4) | 0.71 |
| O11 | 102(7) | 47(2) | 8.9(5) | -16(3) | 1(2) | 1.5(9) | 1.39 |
| O21 | 103(7) | 45(2) | 8.8(5) | 24(3) | -1(2) | -3.2(9) | 1.37 |
| O22 | 163(7) | 28(2) | 8.5(4) | -1(4) | 8(1) | 0(1) | 1.36 |
| O31 | 54(5) | 17(2) | 6.4(4) | 11(3) | 1(1) | -1(1) | 0.73 |
| O32 | 53(5) | 18(2) | 6.0(4) | 14(3) | 0(1) | -1(1) | 0.72 |
| O4 | 71(5) | 23(2) | 6.6(4) | 20(3) | 0(1) | -3(1) | 0.89 |

* β_{ij} is in the expression

$$\exp[-(\beta_{11}h^2 + \beta_{22}k^2 + \beta_{33}l^2 + 2\beta_{12}hk + 2\beta_{13}lh + 2\beta_{23}kl)]$$

Table 5. Site occupancy factors for coexisting oxybiotites 1M and 2M₁

| Site | Mg | Fe* | Ti | Al | Si | |
|-----------------|----|-----------|-------|-------|-------|------------|
| 1M | M1 | 0.624 (6) | 0.190 | 0.0 | 0.186 | |
| | M2 | 0.507 | 0.289 | 0.168 | 0.036 | |
| | T | | 0.024 | 0.0 | 0.266 | 0.71 |
| 2M ₁ | M1 | 0.612 | 0.200 | 0.0 | 0.188 | |
| | M2 | 0.513 | 0.296 | 0.168 | 0.023 | |
| | T1 | | 0.008 | | 0.280 | 0.712 (89) |
| | T2 | | 0.028 | | 0.264 | 0.708 |
| | | | | | | |

* Fe=Fe³⁺+Fe²⁺+Mn

$d(t)$: tetrahedral layer thickness calculated from the z coordinates of basal and apical oxygens of tetrahedra;

$d(i)$: interlayer thickness calculated from the z coordinates of basal oxygens of tetrahedra;

$d(oa)$: octahedral layer thickness calculated from the z coordinates of only the tetrahedral apical oxygens; the $d(oa)$ differs from commonly used octahedral layer thicknesses, $d(oc)$, which are calculated from the z coordinates of all oxygens bonded to the octahedral cations;

$d(h)$: octahedral layer thickness calculated from the z coordinates only of oxygens bonded to hydrogens;

$d(kh)$ K-04 (oxygen bonded to hydrogen) distance along the vector normal to the (001) plane.

It is easy to find the following relations among the d values from the above definitions.

$$d(u) = d(i) + 2d(t) + d(oa) = d(h) + 2d(kh)$$

The calculated d values for the 1M and 2M₁ oxybiotites using the atomic coordinates in Table 4a and 4b, and the cell dimensions in Table 2 are shown in Table 8 together with those for the 1M and 2M₁ hydrogenated oxybiotites using the atomic coordinates given by Takeda and Ross (1975). The value of the difference of d between the oxybiotite and hydrogenated oxybiotite is designated as Δd , and each mean Δd is obtained by averaging the values of Δd for the 1M and 2M₁ polytypes.

Comparison of the structures of oxybiotite and hydrogenated oxybiotite

Role of hydrogen in the biotite structures

The oxybiotite specimens are nearly lacking in hydrogen while the hydrogenated ones contain about 35 percent of the hydroxyl ion. Because the

loss of hydrogen reduces the c edges of the micas, we compared the thicknesses of each layer component to see which one is most responsible for the shortening of the c edges. The d values of the 1M and 2M₁ polytypes are in good agreement with each other within the same species (Table 8). There is a significant difference with respect to d values between oxybiotite and hydrogenated oxybiotite as can be seen in Table 8, where the difference in d values are designated as Δd and each mean Δd is obtained by averaging over 1M and 2M₁ polytypes.

The unit-layer thickness $d(u)$ of the oxybiotite is significantly shorter than that of the hydrogenated oxybiotite, mean $\Delta d(u)$ being 0.063 Å. Among the three mean values of $\Delta d(i)$, $\Delta d(t)$ and $\Delta d(oa)$, which contribute to the mean $\Delta d(u)$, the mean $\Delta d(i)$ is the largest. The difference in c edges between oxybiotite and hydrogenated oxybiotite is about 0.07 Å in

Table 6a. Interatomic distances (Å) and angles (°) for tetrahedral sites of Ruiz Peak oxybiotites

| 1M polytype | | 2M ₁ polytype | | | |
|--------------|------------|--------------------------|--------------------------------|------------|------------|
| T-01 | 1.651(1) | T1-011 | 1.653(2) | T2-011 | 1.648(2) |
| -02 | 1.650(2) | -021 | 1.651(2) | -021 | 1.649(2) |
| -02' | 1.651(2) | -022 | 1.653(2) | -022 | 1.646(2) |
| -03 | 1.668(2) | -031 | 1.667(2) | -032 | 1.670(2) |
| Mean | 1.655(1) | Mean | 1.656(1) | Mean | 1.653(1) |
| | | | (Mean 1.655) | | |
| O1-O2 | 2.678(3) | O11-O21 | 2.686(3) | O11-O21 | 2.676(3) |
| O1-O2' | 2.683(2) | O11-O22 | 2.688(3) | O11-O22 | 2.676(3) |
| O2-O2' | 2.682(1) | O21-O22 | 2.684(3) | O21-O22 | 2.680(3) |
| Mean | 2.681 | Mean | 2.686 | Mean | 2.677 |
| | | | (Mean 2.682) | | |
| O3-O1 | 2.728(3) | O31-O11 | 2.727(3) | O32-O11 | 2.721(3) |
| -02 | 2.720(3) | -021 | 2.723(3) | -021 | 2.722(3) |
| -02' | 2.723(3) | -022 | 2.718(3) | -022 | 2.720(3) |
| Mean | 2.724 | Mean | 2.723 | Mean | 2.721 |
| | | | (Mean 2.722) | | |
| | around T | | around T1 | | around T2 |
| O1-O2 | 108.49(13) | O11-O21 | 108.75(12) | O11-O21 | 108.57(12) |
| O1-O2' | 108.66(13) | O11-O22 | 108.77(11) | O11-O22 | 108.69(11) |
| O2-O2' | 108.68(8) | O21-O22 | 108.65(12) | O21-O22 | 108.88(11) |
| O3-O1 | 110.56(12) | O31-O11 | 110.41(11) | O32-O11 | 110.21(11) |
| -02 | 110.15(10) | -021 | 110.32(11) | -021 | 110.21(11) |
| -02' | 110.26(10) | -022 | 109.88(12) | -022 | 110.24(12) |
| Mean | 109.47 | Mean | 109.46 | Mean | 109.47 |
| | | | | | |
| | T to T' | | T1 to T2 | | |
| around O1 | 137.97(20) | ×4 around O11 | | 138.07(15) | ×4 |
| O2 | 136.45(14) | ×8 O21 | | 136.43(15) | ×4 |
| | | O22 | | 136.62(13) | ×4 |
| Mean | 136.96 | Mean | | 137.04 | |
| | | | | | |
| O2'-O1'-O2'' | 105.52(13) | ×2 O21-O11-O22' | | 105.16(10) | ×2 |
| O1''-O2-O2' | 105.50(13) | ×4 O11-O21'-O22' | | 105.18(10) | ×2 |
| | | O11-O22'-O21 | | 105.13(9) | ×2 |
| Mean | 105.51 | Mean | | 105.16 | |
| | | | | | |
| O2-O1'-O2'' | 134.39(14) | ×2 O21'-O11'-O22' | | 134.81(11) | ×2 |
| O2-O2'-O1' | 134.54(13) | ×4 O11-O21-O22' | | 134.79(11) | ×2 |
| | | O11-O22'-O21' | | 134.92(10) | ×2 |
| Mean | 134.49 | Mean | | 134.84 | |
| | | | | | |
| | | | (tetrahedral rotation angles)* | | |
| α | 7.25 | α | | 7.42 | |
| | | | (Mean 7.34) | | |

*α = |120° - mean(O_b-O_b-O_b) angle| × 0.5

Table 6b. Interatomic distances (Å) and angles (°) for octahedral sites of Ruiz Peak oxybiotites

| 1M polytype | | 2M ₁ polytype | |
|---------------------------------|--------------|--------------------------|--------------|
| <u>M1 octahedron</u> | | | |
| M1-O3 | 2.100 (2) x4 | M1-O31 | 2.099 (2) x2 |
| -O4 | 2.031 (3) x2 | -O32 | 2.093 (2) x2 |
| Mean | 2.077 | -O4 | 2.037 (2) x2 |
| | | Mean | 2.076 |
| (shared edges) | | | |
| O3-O3 | 2.806 (3) x2 | O31-O32' | 2.797 (3) x2 |
| O3-O4 | 2.748 (3) x4 | O31-O4' | 2.758 (3) x2 |
| Mean | 2.767 | O32-O4' | 2.749 (3) x2 |
| | | Mean | 2.768 |
| (unshared edges) | | | |
| O3-O3 | 3.125 (4) x2 | O31-O32 | 3.122 (3) x2 |
| O3-O4 | 3.085 (3) x4 | O31-O4 | 3.083 (3) x2 |
| Mean | 3.098 | O32-O4 | 3.083 (3) x2 |
| | | Mean | 3.096 |
| <u>M2 octahedron</u> | | | |
| M2-O3 | 2.142 (2) x2 | M2-O31 | 2.137 (2) |
| -O3' | 2.088 (2) x2 | -O32' | 2.142 (2) |
| -O4 | 1.947 (2) x2 | +O31' | 2.091 (2) |
| Mean | 2.059 | -O32 | 2.091 (2) |
| | | -O4 | 1.950 (2) |
| | | -O4' | 1.947 (3) |
| | | Mean | 2.060 |
| (shared edges) | | | |
| O3-O3 | 2.780 (4) x2 | O31-O31' | 2.782 (4) |
| O3-O3' | 2.806 (3) x1 | O32-O32' | 2.787 (4) |
| O4-O3 | 2.748 (3) x2 | O31-O32' | 2.797 (3) |
| O4-O4 | 2.656 (5) x1 | O4'-O31 | 2.758 (3) |
| Mean | 2.753 | O4'-O32 | 2.749 (3) |
| | | O4-O4' | 2.657 (4) |
| | | Mean | 2.755 |
| (unshared edges) | | | |
| O3-O3 | 3.044 (2) x2 | O31-O32 | 3.045 (2) |
| O4-O3 | 3.044 (2) x2 | O31'-O32' | 3.045 (2) |
| O4-O3' | 3.089 (3) x2 | O4-O31 | 3.045 (3) |
| Mean | 3.059 | O4'-O32' | 3.047 (3) |
| | | O4-O32 | 3.086 (2) |
| | | O4'-O31' | 3.088 (3) |
| | | Mean | 3.059 |
| (octahedral flattening angles)* | | | |
| Ψ | 56.98 | Ψ | 56.96 |
| | (Mean 56.97) | | |

$$*\sin^2 \Psi = 4 / [3(1+r_0^2)], r_0 = (\text{shared O-O}) / (\text{unshared O-O})$$

the 1M setting and over thirteen times the standard deviation. This difference is comparable with that of the unit-layer thickness $d(u)$, i.e., $\Delta d(u)$. It should be noted that more than two thirds of $\Delta d(u)$ is attributed to $\Delta d(i)$. Thus, the loss or addition of hydrogen atoms mainly affects the interlayer thickness.

This structural change can best be interpreted if the orientation of the O-H bond is known. Although no direct information on the position of the hydrogen atom in the hydrogenated oxybiotite structure has been given from the X-ray data (Takeda and Ross, 1975), it can be predicted from the study of phlogopite structure (Rayner, 1974) by neutron diffraction. The O-H vector of the hydroxyl group is considered to be nearly perpendicular to the plane of the silicate sheets, that is to say the proton is projecting from the octahedral layer towards the positively charged potassium. Since the removal of hydrogen reduces the repulsive force acting be-

tween the interlayer cation and a proton, it is reasonable to postulate that the interlayer cation may move towards the center of the oxygen ring, resulting in a shortening of the interlayer thickness of the oxybiotite structure (Fig. 4).

Because the b edge of the mica layer has been known to affect the interlayer configuration, we first compare the cell dimensions of oxybiotite with those of hydrogenated oxybiotite. The a and b cell edges of the two species in Table 2 reveal that the differences are about 0.01 Å and 0.02 Å respectively, both of which are within five times the standard deviations. The octahedral cation Fe^{2+} is replaced by Fe^{3+} with a small ionic radius in oxybiotite. The mean lengths of the octahedral shared O-O edges averaged over 1M and 2M₁ polytypes of oxybiotite, 2.768 (M1 site) and 2.754 Å (M2 site), are shorter than those of hydrogenated oxybiotite, 2.789 (M1 site) and 2.775 Å (M2 site). However the mean lengths of the unshared edges for the two crystals are not as different, 3.097 and 3.103 Å for the M1 site, and 3.059 and 3.067 Å for the M2 site, respectively. For this reason the cell parameters of the a and b axes are not shortened very much in oxybiotite.

Table 6c. Interatomic distances (Å) for interlayer sites of Ruiz Peak oxybiotites

| 1M polytype | | 2M ₁ polytype | |
|-------------------------------|--------------|--------------------------|--------------|
| (inner) | | | |
| K -O1 | 2.966 (3) x2 | K -O11 | 2.963 (2) x2 |
| -O2 | 2.960 (2) x4 | -O21 | 2.960 (2) x2 |
| Mean | 2.962 | -O22 | 2.958 (2) x2 |
| | | Mean | 2.960 |
| (outer) | | | |
| K -O1 | 3.306 (3) x2 | K -O11 | 3.314 (3) x2 |
| -O2 | 3.288 (2) x4 | -O21 | 3.290 (3) x2 |
| Mean | 3.294 | -O22 | 3.296 (2) x2 |
| | | Mean | 3.300 |
| (lateral) | | | |
| O1-O2 | 4.109 (3) x4 | O11-O11' | 4.129 (5) x1 |
| O2-O2' | 4.107 (4) x2 | O11-O22 | 4.124 (3) x2 |
| Mean | 4.108 | O21-O22 | 4.100 (3) x2 |
| | | O21-O21' | 4.095 (4) x1 |
| | | Mean | 4.112 |
| (basal) | | | |
| O1-O2 | 4.270 (3) x4 | O11-O21 | 4.262 (3) x2 |
| O2-O2' | 4.264 (4) x2 | O11-O22 | 4.257 (3) x2 |
| Mean | 4.268 | O21-O22 | 4.258 (3) x2 |
| | | Mean | 4.259 |
| (shortest interlayer lengths) | | | |
| O1-O1 | 3.339 (6) x2 | O11-O21 | 3.325 (3) x4 |
| O2-O2 | 3.296 (4) x4 | O11-O22 | 3.309 (4) x2 |
| Mean | 3.310 | O22-O22 | 3.320 |
| | | Mean | 3.320 |
| (distances to O4) | | | |
| K -O4 | 3.985 (3) | K -O4 | 3.981 (2) |
| (distances to T sites) | | | |
| K -T | 3.782 (1) x4 | K -T1 | 3.795 (2) x2 |
| -T' | 3.785 (1) x4 | -T2 | 3.794 (1) x2 |
| -T'' | 3.795 (1) x4 | -T1' | 3.783 (1) x2 |
| | | -T2' | 3.782 (1) x2 |
| | | -T1'' | 3.787 (1) x2 |
| | | -T2'' | 3.786 (2) x2 |
| Mean | 3.787 | Mean | 3.788 |

Table 7a. Magnitudes and orientation of thermal ellipsoids of oxybiotite 1M

| Atom | Axis | rms (Å) Displacement | Angle (°) with respect to: | | |
|------|----------------|-------------------------|----------------------------|---------|----------------|
| | | | α | b | $c \sin \beta$ |
| M1 | r ₁ | 0.071(4) | 2(2) | 90 | 92(2) |
| | r ₂ | 0.073(4) | 90 | 180 | 90 |
| | r ₃ | 0.129(3) | 88(2) | 90 | 2(2) |
| M2 | r ₁ | 0.066(2) | 4(1) | 90 | 86(1) |
| | r ₂ | 0.111(2) | 90 | 180 | 90 |
| | r ₃ | 0.125(2) | 94(1) | 90 | 4(1) |
| K | r ₁ | 0.150(4) | 90 | 0 | 90 |
| | r ₂ | 0.152(4) | 178(2) | 90 | 92(2) |
| | r ₃ | 0.194(2) | 92(2) | 90 | 2(2) |
| T | r ₁ | 0.078(2) | 9(16) | 98(17) | 87(1) |
| | r ₂ | 0.083(2) | 98(17) | 172(17) | 90(2) |
| | r ₃ | 0.125(1) | 93(1) | 90(2) | 3(1) |
| O1 | r ₁ | 0.106(5) | 90 | 0 | 90 |
| | r ₂ | 0.137(5) | 134(15) | 90 | 136(15) |
| | r ₃ | 0.152(5) | 136(15) | 90 | 46(15) |
| O2 | r ₁ | 0.104(4) | 28(4) | 62(4) | 89(5) |
| | r ₂ | 0.135(4) | 71(6) | 124(8) | 139(9) |
| | r ₃ | 0.152(3) | 110(4) | 47(7) | 131(9) |
| O3 | r ₁ | 0.078(4) | 126(41) | 37(41) | 87(4) |
| | r ₂ | 0.082(4) | 144(41) | 126(41) | 92(4) |
| | r ₃ | 0.125(3) | 90(3) | 94(4) | 4(4) |
| O4 | r ₁ | 0.088(6) | 1(7) | 90 | 91(7) |
| | r ₂ | 0.097(5) | 90 | 180 | 90 |
| | r ₃ | 0.122(5) | 89(7) | 90 | 1(7) |

The mean inner K–O and mean lateral O–O distances 2.961 and 4.110 Å, for oxybiotites averaged over 1M and 2M₁ polytypes are shorter than those for hydrogenated oxybiotites, 2.972 and 4.146 Å. If the change of interlayer configuration affects the tetrahedral layer configuration, the effect should be seen in differences in the tetrahedral rotation angles α and of the interlayer basal O–O distances. However these differences are not present because the loss of hydrogen atoms in the oxybiotite structure causes the interlayer cation to come closer to the tetrahedral layer resulting in decrease of the interlayer thickness (interlayer separation) without affecting the tetrahedral layer configuration. The mean α angle 7.34° and the mean interlayer basal oxygen distance 4.264 Å for oxybiotites are in good agreement with those for hydrogenated oxybiotites, 7.62° and 4.261 Å, respectively.

The approach of an interlayer cation to the tetrahedral basal oxygen ring would be expected to shorten the K–O4 distance or $d(kh)$, but it does not because the O4 oxygen itself has moved. In spite of the fact that the values of $d(kh)$ for oxybiotites are comparable with those for hydrogenated oxybiotites, the values of $d(h)$ are remarkably different from each other. The absence of the O4–H bonding in oxybiotite gives O4 a residual negative charge which strengthens the bonding of O4 to octahedral

Table 7b. Magnitudes and orientation of thermal ellipsoids of oxybiotite 2M₁

| Atom | Axis | rms (Å) Displacement | Angle (°) with respect to: | | |
|------|----------------|-------------------------|----------------------------|---------|----------------|
| | | | α | b | $c \sin \beta$ |
| M1 | r ₁ | 0.080(3) | 90 | 0 | 90 |
| | r ₂ | 0.085(3) | 176(3) | 90 | 94(3) |
| | r ₃ | 0.120(2) | 94(3) | 90 | 4(3) |
| M2 | r ₁ | 0.072(2) | 124(1) | 35(1) | 99(2) |
| | r ₂ | 0.115(1) | 124(9) | 121(4) | 131(12) |
| | r ₃ | 0.120(1) | 128(8) | 106(6) | 43(11) |
| K | r ₁ | 0.153(2) | 4(2) | 90 | 86(2) |
| | r ₂ | 0.156(2) | 90 | 180 | 90 |
| | r ₃ | 0.189(2) | 94(2) | 90 | 4(2) |
| T1 | r ₁ | 0.076(3) | 134(8) | 44(8) | 94(2) |
| | r ₂ | 0.086(3) | 135(7) | 134(7) | 96(3) |
| | r ₃ | 0.115(2) | 97(2) | 91(3) | 7(2) |
| T2 | r ₁ | 0.080(3) | 139(8) | 50(8) | 99(3) |
| | r ₂ | 0.088(3) | 130(8) | 140(8) | 94(4) |
| | r ₃ | 0.113(2) | 99(2) | 88(4) | 10(2) |
| O11 | r ₁ | 0.112(4) | 27(5) | 64(6) | 84(10) |
| | r ₂ | 0.131(4) | 94(10) | 70(9) | 159(8) |
| | r ₃ | 0.152(4) | 117(4) | 34(6) | 70(8) |
| O21 | r ₁ | 0.103(4) | 145(4) | 55(4) | 90(8) |
| | r ₂ | 0.127(4) | 104(8) | 110(7) | 155(5) |
| | r ₃ | 0.159(4) | 122(3) | 138(4) | 65(5) |
| O22 | r ₁ | 0.109(4) | 89(6) | 4(11) | 86(11) |
| | r ₂ | 0.127(3) | 68(5) | 87(12) | 158(6) |
| | r ₃ | 0.154(3) | 22(6) | 92(4) | 68(6) |
| O31 | r ₁ | 0.067(6) | 132(6) | 42(6) | 88(7) |
| | r ₂ | 0.101(5) | 135(7) | 130(9) | 107(17) |
| | r ₃ | 0.115(4) | 101(11) | 103(14) | 17(17) |
| O32 | r ₁ | 0.064(7) | 135(4) | 45(5) | 90(7) |
| | r ₂ | 0.100(6) | 125(8) | 124(10) | 127(13) |
| | r ₃ | 0.115(5) | 116(8) | 115(10) | 37(13) |
| O4 | r ₁ | 0.069(6) | 133(4) | 44(3) | 83(7) |
| | r ₂ | 0.109(4) | 118(9) | 108(6) | 146(10) |
| | r ₃ | 0.130(5) | 124(6) | 128(4) | 57(9) |

cations, resulting in shortening of $d(h)$ (Fig. 4). The presence of ferric iron in an octahedral cation site in oxybiotite, in contrast with that of ferrous iron in hydrogenated oxybiotite, may shorten $d(h)$ and $d(oa)$ due to the smaller ionic radius. The differences in $d(oa)$ between the two species are much smaller than that of $d(h)$. Hence the difference of $d(h)$ is in large part attributed to the loss or addition of hydrogen atoms. The replacement of ferrous iron by ferric iron has a secondary role.

Octahedral cation ordering in oxybiotites

Partial cation ordering in octahedral sites M1 and M2 is found in the 1M oxybiotite as well as in those of the 2M₁ variety. Mg is enriched in M1, Fe³⁺ preferentially occupies M2, and Ti is present only in M2 (Table 5). The occupancy factor for A1 indicates the enrichment of Al in M1, but this indication is not conclusive because the standard deviation in the occupancy refinement is, 0.1, relatively large.

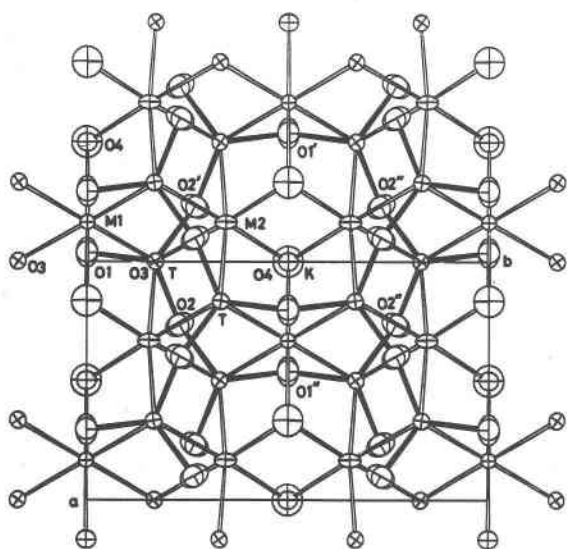


Fig. 1. Projection of the unit-layer structure on (001) for 1M oxybiotite. Ellipsoids enclose 85% probability distribution.

Since this example is the first cation ordering of Mg and Fe found in a common natural trioctahedral mica, there are no data on the ordering of Mg, Fe³⁺ and Ti in micas to compare with the present data. Considering the mode of the ordering of A1 and Li found in fluor-polyolithionite (Takeda and Burnham, 1969) and in lepidolite (Takeda, Haga and Sadanaga, 1971), it is suggested that highly charged cations may have a preference for M2. In xanthophyllite (Takéuchi and Sananaga, 1966), however, the octahedra about M1 are slightly smaller than those about M2; the A1 atoms appear to be incorporated with Mg in M1, while Mg atoms are distributed over the M2 positions.

Hazen and Burnham (1973) found no preference of Fe (mainly consisting of Fe²⁺) for M1 or M2 in annite. Ferrous iron in the hydrogenated oxybiotite (Takeda and Ross, 1975) distributes randomly over the M1 and M2 sites. Preference of Fe for M1 or M2 may depend on whether Fe is in the ferrous or ferric state. Another possible explanation is that the degree of Fe ordering may depend on the temperature of crystallization since the hydrogenated biotite was treated at high temperature for the hydrogenation process.

In any event, it is evident that the Mg, Fe and Ti cations order in the octahedral sites in the oxybiotite, and thus it will be interesting to examine the cation ordering in biotites which contain Mg, Fe or Ti in various ratios.

Compared to those of the M1 site, the thermal ellipsoids of the M2 cations both of oxybiotites 1M

and 2M₁ (Table 7, and Fig. 1 and 2) are more elongated parallel to the *b* directions in the 1M setting. This elongation of the ellipsoid may be ascribed to the positional disorder caused by a little more concentration of Fe³⁺ and Ti in the M2 site than in the M1 site. Since these cations have smaller ionic radius than Mg, the mean M2–O bond length is smaller than the mean M1–O, and the M2 octahedral cation approaches the O4 oxygen (Fig. 4). On the other hand, the cations of Fe³⁺ and Ti have higher charges than Mg, and tend to repel each other. This tendency can give rise to the positional disorder along the line connecting the two nearest M2 sites. This direction of elongation is in agreement with that of the thermal ellipsoids.

Polytypism of oxybiotites 1M and 2M₁

Unit-layer structures

The similarity of the cell dimensions and bond lengths of the 1M and 2M₁ crystals indicates that the two crystals may have similar chemical compositions. The cell dimensions of the 1M polytype agree, within three standard deviations, with those of the 2M₁ polytype in the 1M setting (Table 2). The mean tetrahedral, octahedral, and inner and outer potassium-oxygen bond lengths of the two structures are essentially identical. The comparative values for averaged bond lengths (Table 6) for the 1M and 2M₁ polytypes, respectively, are: tetrahedral (1.655, 1.655Å), octahedral-M1 (2.077, 2.076Å), octahedral-M2 (2.059, 2.060Å), inner K–O (2.962, 2.960Å), and outer K–O (3.294, 3.300Å).

The site occupancy factors of the two structures (Table 5) are essentially identical to each other. The tetrahedral rotation angles (Table 6a), octahedral

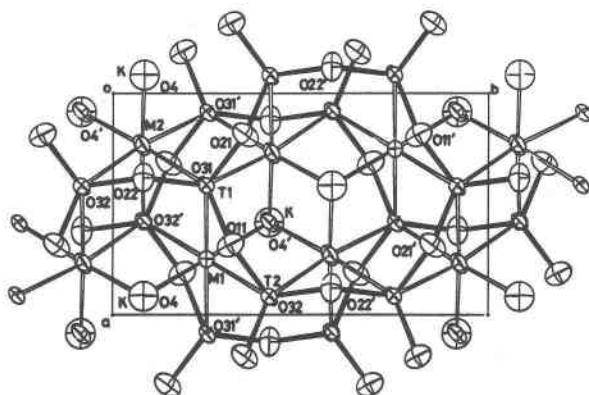


Fig. 2. Projection of the unit-layer structure on (001) for 2M₁ oxybiotite. Ellipsoids enclose 85% probability distribution. The *z* coordinate of M2 is 0.0.

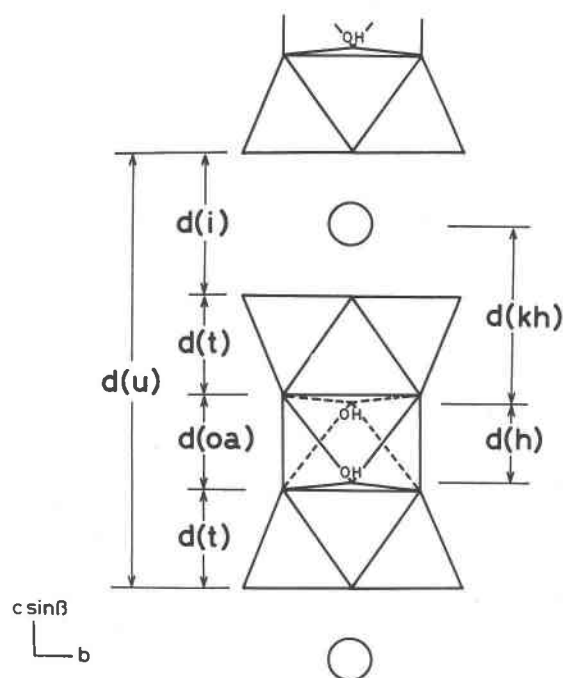


Fig. 3. Definition of d representing various layer thicknesses in mica structure.

flattening angles (Table 6b), and the tiltings of the tetrahedra of the two structures (Table 8) are also identical within the accuracy of the refinements, the tilting of the tetrahedra being not pronounced in either of the polytypes.

A closer examination of Table 6 reveals that the comparative values of each interatomic distance or

angle for the both types are in good agreement with each other. A comparison of the atomic coordinates of the 1M structure with those of the 2M₁ structure converted to the 1M setting (Table 4a) emphasizes that the unit-layer structures are remarkably identical for both types, the maximum departure of the atomic coordinates between the two types being four standard deviations.

It is concluded that the structures of oxybiotites 1M and 2M₁ are ideally polytypic within the accuracy of structure refinements at the present time. The crystals of these two polytypes with similar chemical composition coexist in the same specimen and hence presumably there was no difference in temperature, pressure, and oxygen fugacity of crystallization. The polytypic structures of oxybiotite contrast greatly with the dissimilarities found in the crystal structures of the hydrogenated oxybiotites (Takeda and Ross, 1975) as shown in Figure 5. The difference may be attributed to the presence or absence of hydrogen in the mica structure. In the 2M₁ oxybiotite crystal there may be no strain introduced by the geometrical and atomic restraints associated with stacking, in contrast with the presence of the strain proposed by Takeda and Ross (1975) for 2M₁ polytypes of the hydrogenated oxybiotite.

Effect of the addition of the hydrogen atom to the layer stacking

It has been shown that the unit-layer structures of the coexisting 1M and 2M₁ oxybiotites are identical

Table 8. Layer thicknesses (\AA) of oxybiotites and hydrogenated oxybiotites

| | | $\underline{d}(u)$ | $\underline{d}(i)$ | $\underline{d}(t)$ | $\underline{d}(oa)$ | $\underline{d}(oc)$ | $\underline{d}(h)$ | $\underline{d}(kh)$ | Δz^* |
|-------------------------|-----------------|--------------------|--------------------|--------------------|---------------------|---------------------|--------------------|---------------------|--------------|
| oxybiotite | 1M | 9.947 | 3.287 | 2.241 | 2.178 | 2.111 | 1.978 | 3.985 | 0.021 |
| | 2M ₁ | 9.949 | 3.295 | 2.239 | 2.177 | 2.113 | 1.987 | 3.981 | 0.024 |
| hydrogenated oxybiotite | 1M | 10.013 | 3.334 | 2.244 | 2.191 | 2.138 | 2.033 | 3.990 | 0.014 |
| | 2M ₁ | 10.009 | 3.336 | 2.243 | 2.186 | 2.135 | 2.034 | 3.988 | 0.014 |
| $\Delta \underline{d}$ | 1M | 0.066 | 0.047 | 0.003 | 0.013 | 0.027 | 0.055 | 0.005 | 0.007 |
| | 2M ₁ | 0.060 | 0.041 | 0.004 | 0.009 | 0.022 | 0.047 | 0.007 | 0.010 |
| | Mean | 0.063 | 0.044 | 0.004 | 0.011 | 0.025 | 0.051 | 0.006 | 0.009 |

* Δz : tilting of tetrahedra

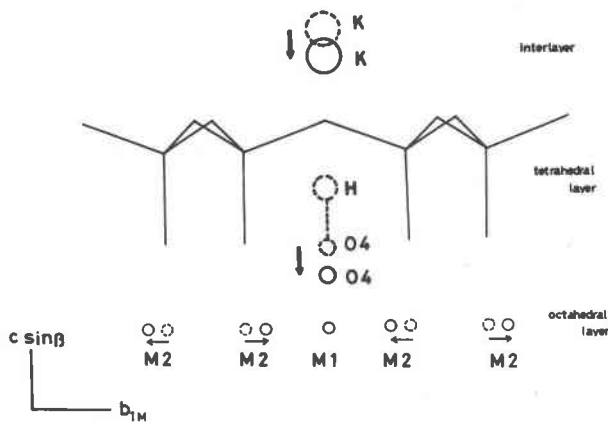


Fig. 4. Schematic diagram showing the effect of the lack of hydrogen and the replacement of Fe²⁺ by Fe³⁺ on the oxybiotite structure. Arrow indicates the direction of the shifts of atoms. Dashed circles are for hydrogenated oxybiotite and open circles are for oxybiotite.

to each other. The study of the structures of 1M and 2M₁ hydrogenated oxybiotites (Takeda and Ross, 1975), however, showed structural dissimilarities with respect to the octahedral configuration between the unit layers of two polytypes. The difference can be summarized by noting that the structure of the unit layer of the 2M₁ polytype is characterized by a shifting, relative to the unit layer of the 1M polytype, of the upper and lower triads of octahedral oxygen atoms as a unit along the $\pm b$ directions. Since the cations in octahedral sites in

the hydrogenated oxybiotite distribute randomly in both polytypes, the structural differences cannot be attributed to the deformation of the octahedra by the different scheme of cation ordering. The presence of a hydrogen atom is considered to be responsible for the structural differences found in the 2M₁ hydrogenated oxybiotite.

The axis of the O-H bond in the structure of 1M phlogopite (Rayner, 1974) is perpendicular to (001) plane. The same orientation is expected to be found in the structure of the 1M hydrogenated oxybiotite because the repulsion forces isotropically acting on a hydrogen atom, as a proton, by the first nearest neighbor cations together with the second and third nearest neighbour cations are considered to be the same for the 1M polytype (Fig. 6a). The hydrogen atom in the 2M₁ structure receives a different (*i.e.* anisotropic) repulsion force especially by the second and third nearest neighbour interlayer cations (Fig. 6b). The anisotropic repulsion force may cause the hydrogen atom to move along the *b* direction in the 2M₁ unit cell away from the position directly under the interlayer K atom. When the hydrogen atom moves towards +*b* direction in this way, the oxygen end of the O4-H bond shifts in the opposite direction -*b* (Fig. 6c). This shift of O4 will cause O31 and O32, which form the triad of octahedral oxygens, to shift in the same direction (Takeda and Ross, 1975).

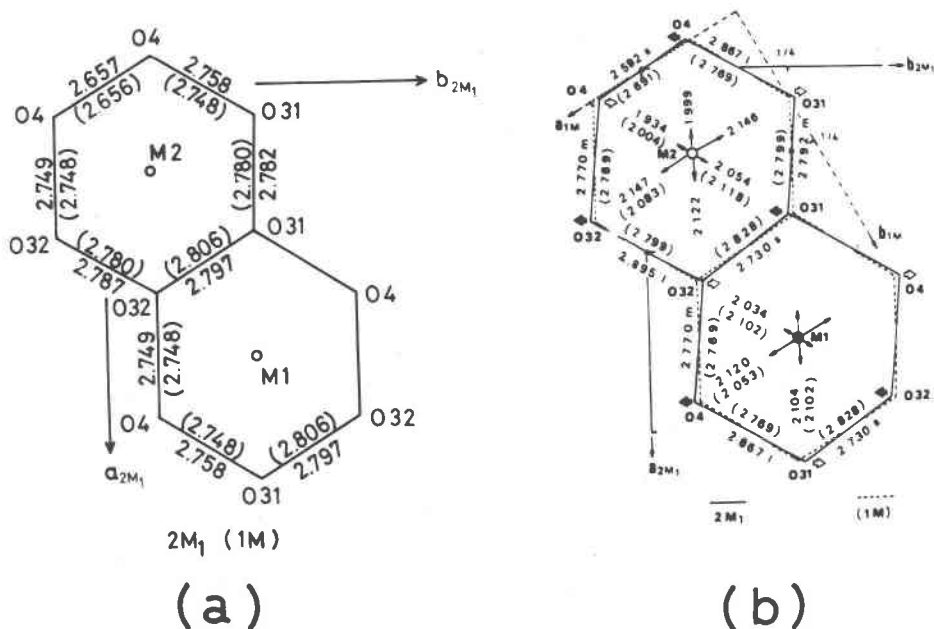


Fig. 5. Projection onto (001) of the M1 and M2 octahedral edges of the 1M (dashed lines) and 2M₁ (solid lines) structures of (a) oxybiotites and (b) hydrogenated-oxybiotites (from Takeda and Ross, 1975). The oxygen-oxygen distances are given, with those of the 1M polytype enclosed in parentheses.

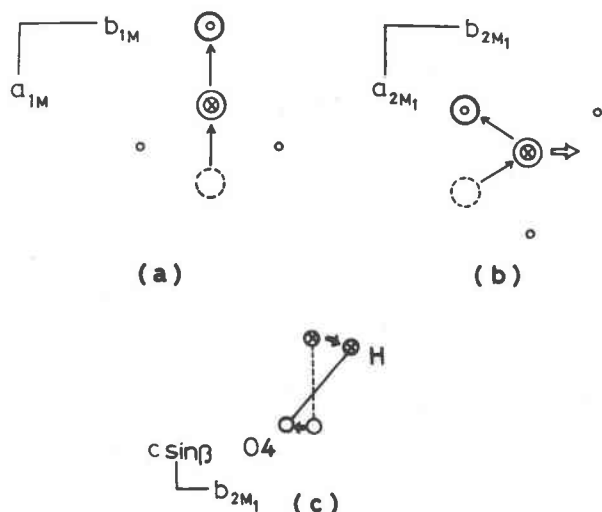


Fig. 6. Schematic diagrams showing the interaction of a hydrogen atom with other cations (a) for the 1M and (b) for the 2M₁ biotites, and (c) showing the tilting of the axis of O-H bond estimated from the 2M₁ biotite structure. Large open circles, dashed ones and open thick ones respectively indicate the first nearest neighbour interlayer cation, the second and the third to the hydrogen atom (middle circle with cross), along the stacking vectors indicated by arrays. Small open circles in (a) and (b) indicate the first nearest octahedral cations. Large open arrow indicates the shift of the hydrogen atom.

Discussion

This study presents information on the structural changes in micas induced by dehydrogenation-hydrogenation reactions due to changing oxygen fugacity. The effect of the lack of hydrogen atoms on mica structures has been elucidated by the comparison of the structures of 1M and 2M₁ oxybiotites with those of the 1M and 2M₁ hydrogenated oxybiotites previously reported.

Because the tetrahedral rotations and the octahedral flattening of the oxybiotites and hydrogenated ones were found to be nearly identical, it can be stated that the lack of hydrogen mainly affects the interlayer configuration and causes the interlayer separation to decrease. This structural change results because the structure is free from the coulomb repulsion between K⁺ and H⁺. A similar aspect, in terms of the interlayer separation, of the replacement of hydroxyl by fluorine in the 1M fluorophlogopite was reported by McCauley, Newnham and Gibbs (1973). Another structural change caused by the addition of hydrogen is exemplified by the 2M₁ hydrogenated oxybiotites (Takeda and Ross, 1975). The structural differences between their unit layers can be interpreted in such a way that the hydrogen atoms interact with the nearest neighboring cations

including not only first and second, but also third nearest neighbors.

With regard to mica polytypism, the comparison of the unit-layer structures of the coexisting 1M and 2M₁ oxybiotites leads to the conclusion that they are ideally polytypic in spite of such complex unit-layer structures as micas. This similarity between the unit layers of the two polytypes is in great contrast with the structural dissimilarities found between the 1M and 2M₁ polytypes of the hydrogenated members. Very precise refinement is required to detect a slight difference between the structures of the oxybiotite polytypes, so that great care was exercised in the refinement. The accuracy is believed to be better than that of the structure refinement of the hydrogenated oxybiotites (Takeda and Ross, 1975).

On the other hand, it has been believed that some structural control may be operative for formation of a regular stacking sequence of such basic polytypes as 1M and 2M₁. A high observation frequency has been noticed for a limited number of short-period polytypes in micas. However, since no remarkable structural dissimilarity, making structural control of stacking sequence possible, was found in the oxybiotites, it is necessary to seek another reason for the predominance of the 1M and 2M₁ polytypes. The offset of the O4 oxygen or fluorine from the potassium position, which was proposed as an interaction controlling polytypism for lepidolite (Takeda, Haga and Sadanaga, 1971), was not found in the oxybiotite. The corrugation of tetrahedra considered as a structural factor controlling stacking sequence in the dioctahedral micas (Güven, 1971) was not found either. The tight configuration around the interlayer cations implies a strong interaction between the neighboring layers. Therefore, this situation coupled with the difference in the second nearest neighbor configuration may produce some forces to propagate the short period for the basic polytypes.

The structural control in oxybiotite may be related to the presence of hydrogen atoms during crystal growth. There is compelling evidence that the crystals may have contained hydrogen atoms when they were crystallized or when the platelet crystal was produced at the initial stage of crystal growth. This is supported by the occurrence description for the oxybiotite from Ruiz Peak (Takeda and Ross, 1975) that the oxidation is inferred to have taken place during and after eruption of the lava in which the oxybiotite occurs. Thus, the mechanism proposed

for the hydrogenated biotites can be applied to the oxybiotites.

Up to now, ditrigonal distortion has been considered to have a primary role on structural control of mica polytypism. Recently, it has been pointed out by Takeda and Morosin (1975) that the ditrigonality may become small, and virtually identical for many micas at high temperature where crystal growth actually took place. The present study shows quantitatively the amount of structural shift induced by the insertion of hydrogen to the mica structure, and suggests that since the electrostatic force acting around the interlayer and the octahedral layer is different due to the loss or addition of hydrogen atoms, it may be more important to consider another structural factor controlling stacking sequence such as the interaction of interlayer cations with hydroxyl ions as suggested by Takéuchi (1965).

Acknowledgments

We thank Dr. M. Ross, U. S. Geological Survey, and Prof. D. R. Wones, Virginia Polytechnic Institute, for providing us with the sample of oxybiotite and for discussion. The computations were performed on HITAC 8800/8700 at the Computer Center of the University of Tokyo. We thank Drs. D. S. McKay, NASA Johnson Space Center, and S. M. Richardson, Iowa State University, for critical reading of the manuscript.

References

- Amelinckx, S. and Dekeyser, W. (1953) Le polytypisme des minéraux micacés et argileux. Première partie: observation et leurs interprétations. *Comptes Rendus XIX International Geological Congress*, 18, 9–22.
- Busing, W. R., Martin, K. O. and Levy, H. A. (1964) ORFFE, a FORTRAN crystallographic function and error program. ORNL-TM-306, Oak Ridge National Laboratory, Oak Ridge, Tennessee.
- Coppens, P. and Hamilton, W. C. (1970) Anisotropic extinction corrections in Zachariasen approximation. *Acta Crystallographica*, A26, 71–83.
- Cromer, D. T. and Mann, J. B. (1968) X-ray scattering factors computed from numerical Hartree-Fock wave functions. *Acta Crystallographica*, A24, 321–324.
- Donnay, G., Donnay, J. D. H. and Takeda, H. (1964) Trioctahedral one-layer micas. II. Prediction of the structure from composition and cell dimensions. *Acta Crystallographica*, 17, 1374–1381.
- Finger, L. W. (1969) Determination of cation distribution by least-squares refinement of single-crystal X-ray data. *Carnegie Institute Washington Year Book*, 67, 216–217.
- Güven, N. (1971) Structural factors controlling stacking sequences in dioctahedral micas. *Clays and Clay Minerals*, 19, 159–165.
- Hazen, R. M. and Burnham, C. W. (1973) The crystal structures of one-layer phlogopite and annite. *American Mineralogist*, 58, 889–900.
- Hazen, R. M. and Wones, D. R. (1972) The effect of cation substitutions on the physical properties of trioctahedral micas. *American Mineralogist*, 57, 103–125.
- Hendricks, S. B. and Jefferson, M. E. (1939) Polymorphism of the micas with optical measurements. *American Mineralogist*, 24, 729–771.
- International Tables for X-ray Crystallography, Vol. 4 (1974) Kynoch Press, Birmingham, England.
- Johnson, C. K. (1965) ORTEP, a FORTRAN thermal ellipsoid plot program for crystal structure illustrations. ORNL-3794, Oak Ridge National Laboratory, Oak Ridge, Tennessee.
- McCauley, J. W., Newnham, R. E. and Gibbs, G. V. (1973) Crystal structure analysis of synthetic fluorophlogopite. *American Mineralogist*, 58, 249–254.
- Miyamoto, M., Takeda, H. and Takano, Y. (1974) Data input language and its compiler for a crystallographic program system. *Science Papers College of General Education, University of Tokyo*, 24, 115–126.
- Ohta, T., Takéuchi, Y. and Takeda, H. (1978) Structural study of brittle micas (II). Statistical mode of stacking sequence in a valuevite crystal as deduced by computer simulation. *Mineralogical Journal*, 9, 1–15.
- Radoslovich, E. W. and Norrish, K. (1962) The cell dimensions and symmetry of layer silicates. I. Some structural considerations. *American Mineralogist*, 47, 599–616.
- Rayner, J. H. (1974) The crystal structure of phlogopite by neutron diffraction. *Mineralogical Magazine*, 39, 850–856.
- Ross, M., Takeda, H. and Wones, D. R. (1966) Mica polytypes: Systematic description and identification. *Science*, 151, 191–193.
- Smith, J. V. and Yoder, H. S. (1956) Experimental and theoretical studies of the mica polymorphs. *Mineralogical Magazine*, 31, 209–235.
- Takeda, H. (1977) Prediction of mica structures at high pressure. (Abstr.) *Crystallography Society of Japan, 1977 Annual Meeting Abstracts*, 2B-10.
- Takeda, H. and Burnham, C. W. (1969) Fluor-polyolithionite: a lithium mica with nearly hexagonal (Si₂O₅)²⁻ ring. *Mineralogical Journal*, 6, 102–109.
- Takeda, H. and Morosin, B. (1975) Comparison of observed and predicted structural parameters of mica at high temperature. *Acta Crystallographica*, B31, 2444–2452.
- Takeda, H. and Ross, M. (1975) Mica polytypism: Dissimilarities in the crystal structures of coexisting 1M and 2M₁ biotite. *American Mineralogist*, 60, 1030–1040.
- Takeda, H., Haga, N. and Sadanaga, R. (1971) Structural investigation of polymorphic transition between 2M₂-, 1M-lepidolite, and 2M₁ muscovite. *Mineralogical Journal*, 6, 203–215.
- Takéuchi, Y. (1965) Structures of brittle micas. *Clays and Clay Minerals, Proceedings of 13th National Conference*, 1–25.
- Takéuchi, Y. and Sadanaga, R. (1959) The crystal structure of xanthophyllite. *Acta Crystallographica*, 12, 945–946.
- Takéuchi, Y. and Sadanaga, R. (1966) Structural studies of brittle micas (I). The structure of xanthophyllite refined. *Mineralogical Journal*, 4, 424–437.
- Wuensch, B. J. and Prewitt, C. T. (1965) Corrections for X-ray absorption by a crystal of arbitrary shape. *Zeitschrift für Kristallographie*, 122, 24–59.